TEST
https://doi.org/10.1007/s11749-024-00952-8

INVITED PAPER

Exploratory functional data analysis

Zhuo Qu[1,2] · Wenlin Dai[3] · Carolina Euan[4] · Ying Sun[1] · Marc G. Genton[1]

Received: 1 October 2023 / Accepted: 8 October 2024

Abstract
With the advance of technology, functional data are being recorded more frequently, whether over one-dimensional or multi-dimensional domains. Due to the high dimensionality and complex features of functional data, exploratory data analysis (EDA) faces significant challenges. To meet the demands of practical applications, researchers have developed various EDA tools, including visualization tools, outlier detection techniques, and clustering methods that can handle diverse types of functional data. This paper offers a comprehensive overview of recent procedures for exploratory functional data analysis (EFDA). It begins by introducing fundamental statistical concepts, such as mean and covariance functions, as well as robust statistics such as the median and quantiles in multivariate functional data. Then, the paper reviews popular visualization methods for functional data, such as the rainbow plot, and various versions of the functional boxplot, each designed to accommodate different features of functional data. In addition to visualization tools, the paper also reviews outlier detection methods, which are commonly integrated with visualization methods to identify anomalous patterns within the data. Finally, the paper focuses on functional data clustering techniques

This research was supported by the King Abdullah University of Science and Technology (KAUST).

✉ Marc G. Genton
marc.genton@kaust.edu.sa

Zhuo Qu
zhuo.qu@kaust.edu.sa; zhuo.qu@stjude.org

Wenlin Dai
wenlin.dai@ruc.edu.cn

Carolina Euan
c.euancampos@lancaster.ac.uk

Ying Sun
ying.sun@kaust.edu.sa

1 Statistics Program, King Abdullah University of Science and Technology, Thuwal 23955-6900, Saudi Arabia

2 Department of Biostatistics, St. Jude Children's Research Hospital, Memphis, Tennessee, USA

3 Center for Applied Statistics, Institute of Statistics and Big Data, Renmin University of China, Beijing 100872, China

4 Department of Mathematics and Statistics, Lancaster University, Lancaster LA1 4YF, UK

Published online: 28 November 2024

which provide another set of practical tools for EFDA. The paper concludes with a brief discussion of future directions for EFDA. All the reviewed methods have been implemented in an R package named EFDA.

Keywords Clustering · Data visualization · Exploratory data analysis · Functional boxplot · Multivariate functional data · Outlier detection

Mathematics Subject Classification 62R10 · 62A09

1 Introduction

Exploratory data analysis (EDA) (Tukey 1977) serves as the primary step in data analysis, exploring basic observed features in a dataset and providing guidelines and diagnostics for statistical modeling. Tukey (1977) contrasts EDA with confirmatory data analysis (CDA) (Tukey 1980), an area of data analysis that is mostly concerned with the techniques of statistical hypothesis testing, confidence intervals, and estimation, to name a few. Overall, EDA can be categorized into data visualization and data mining. The data visualization tools include, but are not limited to, the scatter plot, the histogram, the boxplot (Tukey 1977), and the quantile-quantile plot, whereas data clustering and smoothing are examples of data mining techniques.

When the observations change from univariate/multivariate data to univariate/multivariate functions of an index, such as the time, wavelength, or location index, we call them univariate/multivariate functional data (Ramsay and Dalzell 1991, Ramsay and Silverman 2005). Common real-life examples of univariate functional data include, for instance, raw cell-cycle gene expression curves (Zhao et al. 2004), data from a longitudinal study of the relative diameter and relative height of trees (López-Pintado and Romo 2009), children growth curves (Ramsay and Silverman 2005), petroleum level curves in an oil refinery (Ramsay et al. 2009), daily temperature curves (Qu et al. 2021), annual total precipitation data at 11,918 weather stations from the USA (Sun and Genton 2011, Sun and Genton 2012b), and the directional spectra of sea waves (Euán and Sun 2019, Wu et al. 2023), whereas real-life examples of multivariate functional data include longitudinal hip and knee angle curves for children (Ramsay and Silverman 2005), daily temperature curves derived from data collected by sensors located at different altitudes (Berrendero et al. 2011), coordinates of handwriting data (López-Pintado et al. 2014), hurricane trajectories (Yao et al. 2005, Harris et al. 2021), bivariate daily wind-speed components, namely U and V velocity, mapped in Saudi Arabia (Qu et al. 2021), individual growth velocity curves for different body parts (Carroll et al. 2021), and the joint curves of stunted growth and prevalence of low-birth weight in 77 countries (Qu and Genton 2022).

Mathematically, functional data are considered as realizations of a stochastic process taking values in a Hilbert space. Each realization of the above process is assumed to be independent and to have a continuous sample path. Practically, we can never observe a function entirely over the whole domain, but it can be recorded at certain fixed or random, dense or sparse discrete points, which are either the same or different for each observation. The records can be taken either with or without random measure-

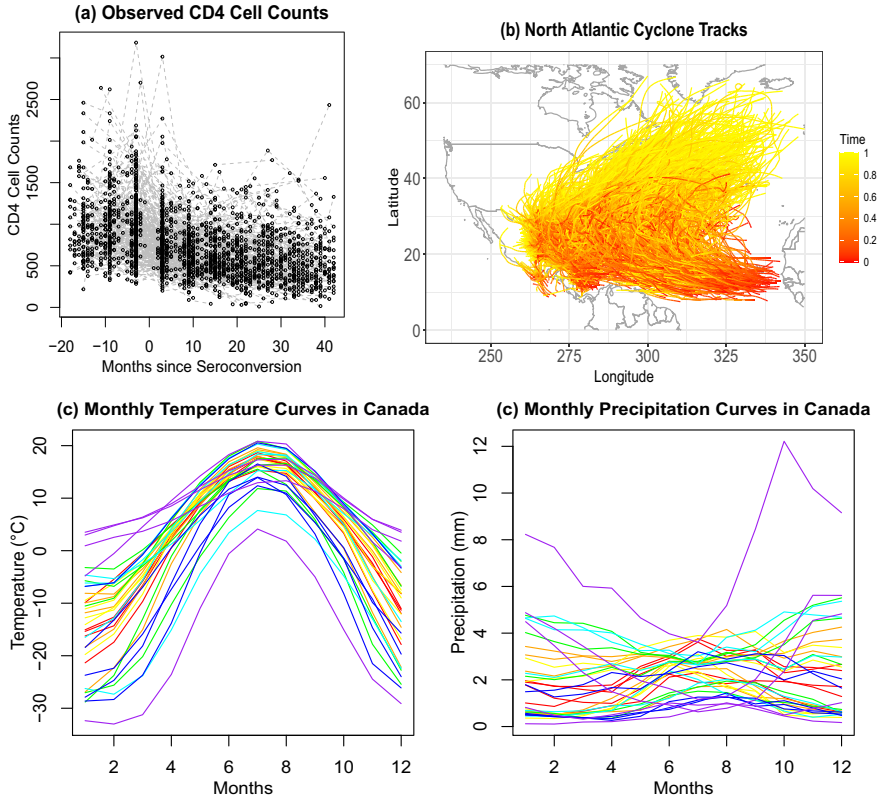

Fig. 1 Various types of functional data: (**a**) observed CD4 counts for 366 samples during months −18 to 42 post seroconversion, (**b**) 1873 North Atlantic cyclone tracks recorded from 1851 to 2021, and (**c**) rainbow plots of monthly temperature and precipitation curves at 35 different locations in Canada averaged over the period from 1960 to 1994. The orderings are based on the modified simplicial band depth (López-Pintado et al. 2014) of Canadian temperature

ment errors. To demonstrate the application of exploratory data analysis methods in diverse scenarios, we will use the following three representative datasets: 1) univariate sparse CD4 cell count data from the R package *refund* (Crainiceanu et al. 2013, see Fig. 1 (a)); 2) bivariate sparse hurricane trajectory data (downloaded online) see Fig. 1 (b); and 3) bivariate dense Canadian daily temperature and precipitation curves from the R package *fda* (Ramsay et al. 2023, see Fig. 1 (c).

Functional data can be regarded as a natural extension of a vector from finite dimension to infinite dimension. However, with the continuing development of data collection techniques, functional observations present themselves more frequently. Hence, functional data analysis (FDA) (Ramsay et al. 2009) includes both an intrinsic and an applied interest. The intrinsically infinite dimension of functional data poses challenges for the existing visualization tools as well as for the exploratory analysis procedures applied to the data. During the past two decades, much effort has been made to find effective inference methods for functional data, such as estimating mean

and covariance functions (Yao et al. 2005, Wang et al. 2016, Happ and Greven 2018). A series of methods and tools have been developed, along with the proliferation of statistical models and inference techniques for functional data (Ramsay and Silverman 2005, Horváth and Kokoszka 2012, Wang et al. 2016).

Despite the importance of EDA for real-data applications, there is no systematic review of EDA for functional data. The goal of this paper is to provide a comprehensive review of recent EDA methods for functional data to which we refer as EFDA. We first review the novel data mining methodology and visualization tools specifically used for FDA as an initial step prior to diving into modeling and statistical inference analysis. As compared to a case study in exploratory functional data analysis (Sangalli et al. 2009), we introduce EFDA with novel visualization tools and methods of clustering. In addition, we use the univariate sparse CD4 data, the bivariate irregular North Atlantic cyclone track data, and the bivariate dense Canadian weather data to illustrate different methods. In contrast to the review of Wang et al. (2016), which concerns the general analysis of univariate functional data, we cover the EDA of p-dimensional ($p \in \mathbb{Z}_+$) functional data, where the measurement index per sample can vary. Hence, univariate functional data correspond to the special case of $p = 1$, and samples with dense grid points correspond to the special case of identical measurement indexes. In contrast to the visualization review by Genton and Sun (2020), we delve into more recent visualization tools that encompass a broader range of functional data. Additionally, we provide a comprehensive overview of clustering methods for EFDA, showcasing their integration with visualization tools.

The rest of the paper is organized as follows. Section 2 summarizes descriptive statistics for functional data. Section 3 reviews current tools for visualizing the observed functional data intuitively. Section 4 displays visualization tools featuring the descriptive statistics of functional observations. Section 5 presents several methods for functional data clustering of dense and sparse functional data, separately. Section 6 concludes the paper with a summary and discussion. An R package named EFDA has been developed to facilitate practical exploratory functional data analysis.

2 Notations and functional descriptive statistics

In this section, we focus on the mathematical definitions and basic descriptive statistics of functional data, with an emphasis on the case in which the dataset is contaminated by abnormal observations (outliers).

2.1 Notations

Let $\boldsymbol{Y}$ be a functional random vector (Hsing and Eubank 2015) with each component taking values in an infinite-dimensional space. Without loss of generality, we allow each marginal random vector in a p-variate stochastic process $\boldsymbol{Y}(\boldsymbol{t})$ to be defined at different indexes, that is, $\boldsymbol{Y}(\boldsymbol{t}) = (Y^{(1)}(t^{(1)}), \ldots, Y^{(p)}(t^{(p)}))^\top$ with $\boldsymbol{t}^\top := (t^{(1)}, \ldots, t^{(p)}) \in \mathcal{T} := \mathcal{T}_1 \times \cdots \times \mathcal{T}_p \subset \mathbb{R}^p$. Note that $\boldsymbol{t}$ is a p-dimensional vector, with its element $t^{(j)}$ being a random design point and independent of all

other random variables. Each element $Y^{(j)}(t^{(j)})$ $(j = 1, \ldots, p)$ is defined on the domain $\mathcal{T}_j$, where the $\mathcal{T}_j$s are compact sets in $\mathbb{R}$ with finite Lebesgue measures. In brief, $Y^{(j)}(t^{(j)})$: $\mathcal{T}_j \to \mathbb{R}$ is assumed to be square-integrable in $\mathcal{T}_j$, denoted as $L^2(\mathcal{T}_j)$. Then, we consider the p-dimensional functional data $\boldsymbol{Y} = \{\boldsymbol{Y}(\boldsymbol{t})\}_{\boldsymbol{t}\in\mathcal{T}}$ as sample paths of the stochastic process $\boldsymbol{Y}(\boldsymbol{t})$, and we have $\boldsymbol{Y} \in \mathcal{H}$, where the space $\mathcal{H} := L^2(\mathcal{T}_1) \times \cdots \times L^2(\mathcal{T}_p)$. Let $\boldsymbol{Y}_1, \ldots, \boldsymbol{Y}_N$ be a set of independent realizations of $\boldsymbol{Y}$. Suppose the j-th component in the b-th sample, $Y_b^{(j)}$, is observed at $L_b^{(j)}$ time points, $t_{b,u}^{(j)}$, where $b = 1, \ldots, N$, and $u = 1, \ldots, L_b^{(j)}$. When $p = 1$, we return to univariate functional data, and $\boldsymbol{Y} \in \mathcal{H}$, where the space $\mathcal{H} := L^2(\mathcal{T})$ and $\mathcal{T} \subset \mathbb{R}$.

2.2 Moment-based descriptive statistics

Define $\boldsymbol{\mu}(\boldsymbol{t}) := \mathrm{E}\{\boldsymbol{Y}(\boldsymbol{t})\}$ as the population mean function $\boldsymbol{\mu}$ evaluated at point $\boldsymbol{t}$. Then, the sample mean of the jth component of $\boldsymbol{Y}$ at $t_l^{(j)}$ is $\hat{\mu}^{(j)}(t_l^{(j)}) = \frac{\sum_{b=1}^{N}\sum_{u=1}^{L_b^{(j)}} Y_b^{(j)}(t_{b,u}^{(j)})\mathrm{I}(t_{b,u}^{(j)}=t_l^{(j)})}{\sum_{b=1}^{N}\sum_{u=1}^{L_b^{(j)}} \mathrm{I}(t_{b,u}^{(j)}=t_l^{(j)})}$ for $j = 1, \ldots, p$ and $l = 1, \ldots, L$, where L is the total number of evaluated time points and $\mathrm{I}(\cdot)$ is the indicator function. When functional data all have common and finite grid points, the number of observations at each grid point is equal to the number of functional samples. However, when functional data are observed on irregular grids, the number of observations at each grid point varies and is imbalanced. It may be practical to count the number of observations in bins rather than at each grid point. To obtain the whole curve, one can simply apply smooth interpolation or nonparametric smoothing methods, e.g., kernel smoothing (Wand and Jones 1995), local polynomial smoothing (Fan and Gijbels 1996), principal component analysis (Yao et al. 2005), or spline smoothing (Wang 2011).

For $\boldsymbol{s}, \boldsymbol{t} \in \mathcal{T}$, we define the matrix of covariances $\boldsymbol{\Sigma}(\boldsymbol{s}, \boldsymbol{t}) := \mathrm{cov}\{\boldsymbol{Y}(\boldsymbol{s}), \boldsymbol{Y}(\boldsymbol{t})\}$ with elements $\Sigma_{ij}(s^{(i)}, t^{(j)}) := \mathrm{cov}\{Y^{(i)}(s^{(i)}), Y^{(j)}(t^{(j)})\}$ for $s^{(i)} \in \mathcal{T}_i$, $t^{(j)} \in \mathcal{T}_j$,$i, j = 1, \ldots, p$. Likewise, the pointwise covariance function can be estimated as

$$\hat{\Sigma}_{ij}(t_k^{(i)}, t_l^{(j)}) = \frac{\sum_{b=1}^{N}\sum_{u=1}^{L_b^{(i)}}\sum_{v=1}^{L_b^{(j)}}\{Y_b^{(i)}(t_{b,u}^{(i)}) - \hat{\mu}^{(i)}(t_k^{(i)})\}\{Y_b^{(j)}(t_{b,v}^{(j)}) - \hat{\mu}^{(j)}(t_l^{(j)})\}\mathrm{I}(t_{b,u}^{(i)} = t_k^{(i)}, t_{b,v}^{(j)} = t_l^{(j)})}{\sum_{b=1}^{N}\sum_{u=1}^{L_b^{(i)}}\sum_{v=1}^{L_b^{(j)}}\mathrm{I}(t_{b,u}^{(i)} = t_k^{(i)}, t_{b,v}^{(j)} = t_l^{(j)})},$$

and the whole surface of the covariance function can be obtained by smoothing the three-dimensional (3D) scatterplot. Common reconstruction methods for sparse functional data include multivariate functional principal component analysis (MFPCA) (Happ and Greven 2018) and tensor-product splines (Cai and Yuan 2010, Xiao et al. 2018, Li et al. 2020). Practically, these records are often assumed to be contaminated by measurement errors, and we refer the readers to Wang et al. (2016) for a comprehensive review of the estimation of mean and covariance functions in such a scenario.

2.3 Robust methods

Functional data can be contaminated by abnormal observations, also known as outliers, in a similar manner to univariate or multivariate data. Outliers may severely bias the aforementioned moment-based estimators and, consequently, lead to incorrect inference results. Hence, it is desirable to develop methods that can reduce/eliminate the influence of outliers and summarize functional data robustly.

For univariate data, order-statistics and ranks induced naturally by the order of scalars on the real line are commonly used to design robust analysis methods, whereas for functional data, such a natural ranking is not available. During the past two decades, the idea of data depth, initially proposed to rank multivariate data, has been generalized to functional data. Specifically, a functional depth, taking values in [0, 1], maps functional data to scalars. It evaluates functional data by assigning larger depth values to central functions and smaller depth values to the more outward ones. Consequently, these scalars provide a ranking criterion for functional data from the center outward.

Commonly implemented depth notions for dense univariate functional data include, but are not limited to, band depth (BD) and modified band depth (MBD) (López-Pintado and Romo 2009, Sun et al. 2012), half-region depth and modified half-region depth (HRD and MHRD) (López-Pintado and Romo 2011), extremal depth (Narisetty and Nair 2016), functional tangential angle pseudo-depth (FUNTA) (Kuhnt and Rehage 2016) and its robustified version, order extended integrated depth (Nagy et al. 2017), spatial depth (Serfling and Wijesuriya 2017), total variation depth (TVD) (Huang and Sun 2019a), and elastic depths (Harris et al. 2021). For dense multivariate functional data, available depth notions include combinations of univariate functional depth measures (Ieva and Paganoni 2013), simplicial band depth (SBD) and modified simplicial band depth (MSBD) (López-Pintado et al. 2014), multivariate functional halfspace depth (MFHD) (Claeskens et al. 2014), and multivariate FUNTA pseudo-depth and its robustified version (Kuhnt and Rehage 2016).

For sparse univariate functional data, López-Pintado and Wei (2011) first proposed a model-based consistent procedure for estimating the depths based on the estimated curves on regular grids. Then, Sguera and López-Pintado (2021) proposed a new depth that enables the curve estimation uncertainty to be incorporated into the depth analysis. Those two depth notions have been extended to sparse multivariate functional data by Qu and Genton (2022), who also compared their ranking performances with simulations. Elías et al. (2023) proposed an integrated functional depth for partially observed functional data, but this depth does not work if the data are not on a common domain or all samples show missing values. In a recent study, Qu et al. (2022) introduced a novel framework for multivariate functional depths, specifically designed for sparse multivariate functional data and eliminating the need for curve estimation. This new depth concept, termed "global depth," distinguishes itself from previous approaches by handling sparse functional data directly. The authors have demonstrated how the procedures for MFHD and multivariate extremal depth (an extension of extremal depth) can be adapted to their global depth framework.

Functional depths provide a natural basis for defining the median, extremes, and quantiles of functional data. Fraiman and Muniz (2001) defined the functional median

as the deepest observation, i.e., the sample with the largest depth value, denoted as $\boldsymbol{M} = \arg\max_{\boldsymbol{Y}} D(\boldsymbol{Y}, F_{\boldsymbol{Y}})$, where $D(\boldsymbol{Y}, F_{\boldsymbol{Y}})$ is the depth of a random function $\boldsymbol{Y}$ with respect to its distribution $F_{\boldsymbol{Y}}$.

The functional version of the α-trimmed mean, $\boldsymbol{\mu}_\alpha$, is defined as the average of the deepest $1-\alpha$ proportion,

$$\boldsymbol{\mu}_\alpha = \frac{\mathrm{E}[\boldsymbol{Y} \cdot \mathrm{I}(D(\boldsymbol{Y}, F_{\boldsymbol{Y}}) \in [\beta, \infty))]}{\mathrm{E}[\mathrm{I}(D(\boldsymbol{Y}, F_{\boldsymbol{Y}}) \in [\beta, \infty))]},$$

where β is such that $\mathrm{E}(\mathrm{I}[D(\boldsymbol{Y}, F_{\boldsymbol{Y}}) \in [\beta, \infty))] = 1-\alpha$. The empirical definitions of these two statistics can be expressed as

$$\hat{\boldsymbol{M}}_N = \arg\max_{i=1,\ldots,N} D(\boldsymbol{Y}_i, \hat{F}_{\boldsymbol{Y}}) \quad \text{and} \quad \hat{\boldsymbol{\mu}}_{\alpha,N} = \frac{\sum_{i=1}^N \boldsymbol{Y}_i \cdot \mathrm{I}(D(\boldsymbol{Y}_i, \hat{F}_{\boldsymbol{Y}}) \in [\beta, \infty))}{\sum_{i=1}^N \mathrm{I}(D(\boldsymbol{Y}_i, \hat{F}_{\boldsymbol{Y}}) \in [\beta, \infty))},$$

where $\hat{F}_{\boldsymbol{Y}}$ denotes the empirical distribution function.

Likewise, the α-trimmed covariance function can be defined as

$$\Sigma_{i,j;\alpha}(s^{(i)}, t^{(j)}) = \frac{\mathrm{E}[\{Y^{(i)}(s^{(i)}) - \mu_\alpha^{(i)}(s^{(i)})\}\{Y^{(j)}(t^{(j)}) - \mu_\alpha^{(j)}(t^{(j)})\}\mathrm{I}(D(\boldsymbol{Y}, F_{\boldsymbol{Y}}) \in [\beta, \infty))]}{\mathrm{E}[\mathrm{I}(D(\boldsymbol{Y}, F_{\boldsymbol{Y}}) \in [\beta, \infty))]}$$

for $s^{(i)} \in \mathcal{T}_i$ and $t^{(j)} \in \mathcal{T}_j$ and $i, j = 1, \ldots, p$, and its empirical version can be derived by substituting the statistics with their respective estimators.

For univariate functional data, e.g., the jth component of multivariate functional data ($j = 1, \ldots, p$), another concept related to data ranking is the $1-\alpha$ central region, which contains $100(1-\alpha)\%$ of the deepest data (López-Pintado and Romo 2009). In Sun and Genton (2011), the 50% central region is visualized as the central box in the functional boxplot. Moreover, Narisetty and Nair (2016) defined the central region as

$$\boldsymbol{C}_{1-\alpha}^{(j)} = \{Y^{(j)} \in L^2(\mathcal{T}_j) : Y_L^{(j)}(t^{(j)}) \le Y^{(j)}(t^{(j)}) \le Y_U^{(j)}(t^{(j)}),\ \forall t^{(j)} \in \mathcal{T}_j\},$$
$$j = 1, \ldots, p,$$

where $Y_L^{(j)}$ and $Y_U^{(j)}$ are lower and upper α-envelope functions, $Y_L^{(j)} = \inf\{Y^{(j)} \in L^2(\mathcal{T}_j) : D(Y^{(j)}, F_{Y^{(j)}}) > \alpha\}$ and $Y_U^{(j)} = \sup\{Y^{(j)} \in L^2(\mathcal{T}_j) : D(Y^{(j)}, F_{Y^{(j)}}) > \alpha\}$, respectively. It was shown that compared to other depth notions, the extremal depth-based central region achieves the nominal coverage probability. A similar concept of global envelope was developed by Myllymäki et al. (2017) for testing spatial processes and extensively discussed in Myllymäki and Mrkvička (2019).

3 Direct visualization of functional observations

Visualization (Friedman et al. 2002) has long been a component of great importance to EDA, and many visualization tools are widely used as routine steps in the analysis

procedure. For instance, the histogram of a univariate dataset shows a rough sense of the density of its underlying distribution, the scatter plot of a bivariate dataset presents the locations of the data points on a two-dimensional plane to provide some idea of the relation between the two variables, and a heatmap depicts the magnitude of an observation as color in two dimensions. Similar demands in FDA motivate researchers to develop new graphical tools.

Here, we highlight several reasonably simple tools that have proved useful in the literature (Hyndman and Shang 2010, Hubert et al. 2015, Wrobel and Goldsmith 2016). We will consider the Canadian weather dataset from Fig. 1 (c) as one illustrative example. This dataset includes monthly recorded temperature and precipitation curves for 35 stations in Canada over the period from 1960 to 1994.

3.1 Spaghetti plot and rainbow plot

A spaghetti plot (Allen 2019) is a simple visualization that assigns a distinct color to each observation, making it easy to track movement for data with small sample sizes. However, such a plot may look messy when used to visualize big functional datasets. The rainbow plot, proposed by Hyndman and Shang (2010), can be regarded as an improvement of the spaghetti plot. As a visualization of all the curves, it adds a data ordering feature and colors the observations based on the ordering, using the rainbow palette. The order can reflect time, data depth, data density, or another index.

In Fig. 1 (c), the Canadian temperature curves are ordered with the MSBD from the median to the extremes, and the curves are labeled from red to purple in the rainbow palette. We can see that the red group represents the median tendency of the temperature and precipitation over the course of a year, whereas the purple group includes data from some stations with high temperatures and high precipitation during winter and some stations with low temperatures and low precipitation all year round.

3.2 Heatmap

A heatmap (Hubert et al. 2015) represents different values by using a system of color-coding. In FDA, an $n \times m$ heatmap is suitable for showing a functional dataset consisting of n curves recorded on m common design points.

We visualize the data with a heatmap in Fig. 2. For instance, each cell in Fig. 2 (a) represents the average temperature at one station in a specific month, each row represents the monthly average temperature curve for a station, and each column represents the average temperature at 35 stations in a particular month. Some abnormal information can be easily detected through the heatmap. Figure 2 (a) shows that Victoria and Vancouver have persistent high temperatures between April and October, whereas temperatures in Resolute and Iqaluit remain below 10 degrees Celsius almost all year round. Pr. Rupert has monthly precipitation up to 6 mm, except between April and August, whereas the other stations have monthly precipitation of less than 6 mm. We

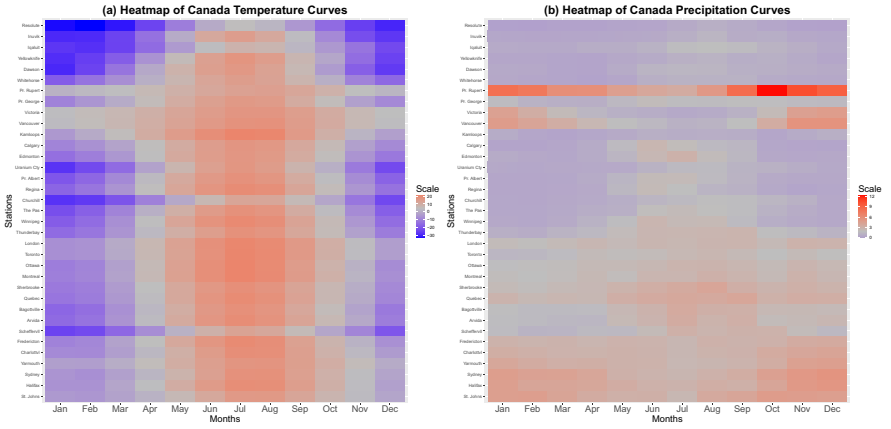

Fig. 2 Heatmap of 35 Canadian monthly average temperature (**a**) and precipitation (**b**) curves over the period from 1960 to 1994

refer the readers to Shang and Hyndman (2017) and Parkinson et al. (2020) for more examples.

3.3 Interactive plots

Several packages have been developed to generate interactive visualization for functional data. An interactive plot retains the advantages of both visual and numerical illustration of data, i.e., it is intuitive as well as accurate. The interaction can be achieved in many ways, e.g., by showing the associated records at the locations indicated by the cursor, zooming in or out, or interacting between different plots. Wrobel et al. (2016) proposed using the *refund.shiny* package (2022) that creates interactive graphics for FDA. The *refund.shiny* package relies on the *shiny* package (Chang et al. 2015) to generate such an interactive user interface. Figure 3 illustrates the observed scores for the functional principal components and the corresponding fitted values for each station in the Canadian temperature data. Another commonly used tool is the *plotly* package 2018), which produces interactive plots with two or three dimensions in combination with a web portal.

3.4 Animations

An animation (or video) is another powerful tool for enhancing still figures that can visualize the dynamic evolution of data. Genton et al. (2015) proposed the term *visuanimation* for referring to visualization through animations, and they explored the utility of animation in various perspectives of statistics. Castruccio et al. (2019) illustrated predicted global temperature data, which can be regarded as functional data, varying spatially and temporally via a 3D virtual-reality movie, and they developed a mobile application that enables users to watch the movie interactively.

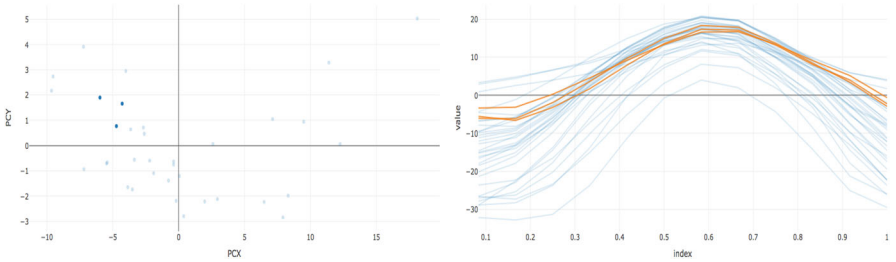

Fig. 3 An illustration of an interactive functional principal component (FPC) plot generated by the *refund.shiny* package. The left panel shows the observed score scatterplot for selected FPCs of Canadian temperature data, and the right panel shows fitted curves, where the three in orange were selected in the left panel and the others are in light blue (color figure online)

4 Visualization with functional summary statistics

Many visualization tools for classical data have been developed to feature descriptive statistics. For instance, the boxplot (Tukey 1977) of a univariate dataset illustrates the structure of the data by showing their descriptive statistics, e.g., the median, quartiles, extreme values, and possible outliers. The bagplot (Rousseeuw et al. 1999) of a bivariate dataset presents the deepest data point, the deepest 50% of the data points, and possible outliers under the ranks given by the halfspace depth (Tukey 1975). In FDA, functional data can be transformed to values of depth or outlyingness (Dai and Genton 2019) from the center outwards (see Subsection 2.3) for visualization and outlier detection. Hence, we will introduce visualization tools that contain functional summary statistics of raw data.

4.1 Visualization based on ranking information

Hyndman and Shang (2010) first proposed several visualization tools for smoothed functional data, such as the rainbow plot, functional bagplot, and functional highest density region (HDR) boxplot available in the R package *rainbow* (Shang and Hyndman 2019). The rainbow plot is a simple visualization of all the data with the only added feature being a rainbow color palette based on an ordering of data. The rainbow plot allows for exploration across metrics like depth, density, or chronological order. The functional bagplot is based on the bivariate bagplot of Rousseeuw et al. (1999). It first applies the bivariate bagplot to the first two robust functional principal component scores as an auxiliary tool to rank the observations and detect outliers. Then, it displays the median curve, the 50% inner region, and the 99% fence. Curves that are partially outside these regions are identified as outliers. The functional HDR boxplot is a mapping of the bivariate HDR boxplot (Hyndman 1996) of the first two robust functional principal component scores to the functional curves. In contrast to the functional bagplot, this method displays curves with high HDRs. Specifically, it focuses on curves whose first two functional principal component scores correspond to the 50% inner and 95% outer bivariate HDRs. Additionally, it identifies outliers as points that are excluded from the 95% outer HDR.

The functional boxplot, as proposed by Sun and Genton (2011), is a data visualization technique used to summarize the distribution and features of a set of functional data. It uses the functional depth and highlights the central quantiles and possible outliers. Analogous to the classical boxplot, there are four descriptive statistics in the functional boxplot (see Fig. 4): the envelope of the 50% central region, the median curve, the outliers, and the maximum non-outlying envelope. An observation is flagged as an outlier if its measurement at any grid point is outside a constant factor times the range at the central region. The constant factor is set to be 1.5 under the assumption that observations at each index are independent and identically distributed and that they follow a normal distribution. The functional boxplot is generalized to other types of boxplots to suit functional data with additional characteristics. We can categorize various functional boxplots as follows: those tailored for independent and dense grid data, those designed for spatiotemporal data, those handling missing data, and those catering to more general observations.

In the first category, the enhanced functional boxplot (Sun and Genton 2011), the double-fence functional boxplot (Serfling and Wijesuriya 2017), and the two-stage functional boxplot (Dai and Genton 2018a) were proposed to underline more features. For instance, the enhanced functional boxplot provides 25% and 75% central regions on the basis of the functional boxplot and the two-stage functional boxplot; the double-fence functional boxplot includes an additional fence of 0.5 interquartile regions, enhancing its ability to identify specific shape and location outliers. Comparatively, the two-stage functional boxplot initially employs directional outlyingness, as proposed by Dai and Genton (2019), to detect outliers using the robust Mahalanobis distance of functions with Rousseeuw (1985)'s minimum covariance determinant estimators. Outliers with distances larger than the cutoff value, determined from the findings in Hardin and Rocke (2005), are then colored in green. Subsequently, the remaining curves undergo processing through a functional boxplot. Figure 4 illustrates these tools on the CD4 functional data.

In the second category, the adjusted functional boxplot (Sun and Genton 2012a) and surface boxplot (Genton et al. 2014) were proposed for use with spatiotemporal data. The spatiotemporal data can be viewed as a temporal curve at each spatial location or as a spatial surface at each time. In the former case, correlations need to be considered across locations. Hence, Sun and Genton (2012a) proposed the adjusted functional boxplot, which flexibly selects the constant factor to control the probability of correctly detecting no outliers. In the aforementioned work, Genton et al. (2014) extended the concept of MBD to modified volume depth specifically for image data. This extension enabled them to introduce a surface boxplot, which facilitates the visualization of images based on the modified volume depth. Similarly, the same four descriptive statistics can also be established by using the modified volume depth. López-Pintado and Wrobel (2017) proposed multivariate volume depth (MVD) to rank images from the center outwards. Furthermore, Huang and Sun (2019b) and Huang et al. (2023) adapted the functional boxplot method to visualize test functions of covariance properties for univariate and multivariate spatiotemporal random fields. This was further extended by Jiménez-Varón et al. (2023) to the visualization of copula symmetry.

In the third category, the sparse functional boxplot and the intensity sparse functional boxplot (Qu and Genton 2022) were proposed for visualization. Data

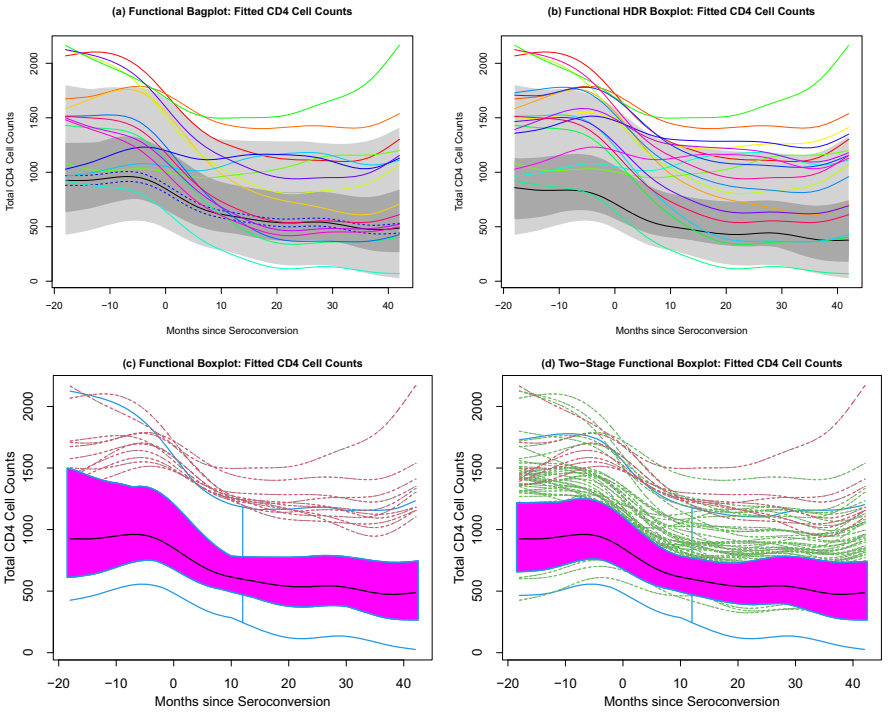

Fig. 4 Comparisons of the functional bagplot, the functional HDR boxplot, and the functional boxplots of the fitted CD4 cell counts from bootstrap MFPCA (Qu and Genton 2022): (**a**) the functional bagplot, (**b**) the functional high-density region (HDR) boxplot, (**c**) the functional boxplot, and (**d**) the two-stage functional boxplot

reconstruction is required with MFPCA (Happ and Greven 2018). In addition to the descriptive statistics in the functional boxplot, the sparse functional boxplot displays the smooth sparseness proportion within the 50% central region, and the intensity sparse functional boxplot displays the intensity of the smooth sparseness within the 50% central region. Usually, the directional outlyingness (Dai and Genton 2019) and sparse functional boxplots are combined to form the sparse two-stage functional boxplot and the intensity sparse two-stage functional boxplot for visualization and outlier detection (see Fig. 5). In the sparse functional boxplot and its two-stage forms in Fig. 5 (a)-(b), the gray shading denotes the proportion of missing data within the central region, while the magenta shading indicates the observed data proportion within the same region. In the intensity sparse functional boxplot and its two-stage forms in Fig. 5 (c)-(d), the central region reflects the intensity of sparseness, with magenta representing the least sparseness intensity and white indicating the highest sparseness intensity. Outliers are visualized with the observed portion shown in red or green (detected from the functional boxplot or directional outlyingness, respectively) and the missing portion in gray.

Furthermore, sparse functional boxplots have been extended to the simplified sparse functional boxplot (Qu et al. 2022) and the simplified intensity sparse functional

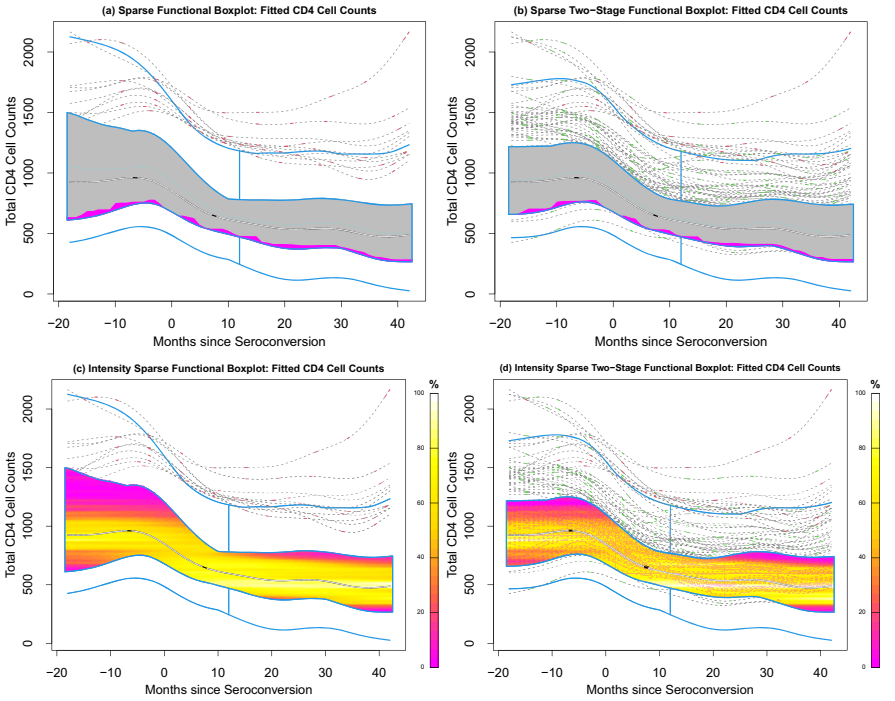

Fig. 5 Functional boxplot and its variations when missing values exist, taking the instance of the fitted CD4 cell counts from bootstrap MFPCA (Qu and Genton 2022). The left column includes (**a**) the sparse functional boxplot and (**c**) the intensity sparse functional boxplot. The right column includes (**b**) the sparse two-stage functional boxplot and (**d**) the intensity sparse two-stage functional boxplot

boxplot without data reconstruction. The simplified visualization tools are based on the global multivariate functional depths (Qu et al. 2022), which are applied to the sparse multivariate functional data directly without data reconstruction.

The fourth category includes other natural extensions of the functional boxplot for data expressed as sets, curves, paths, or trajectories. Whitaker et al. (2013) defined the set band depth and introduced a contour boxplot for visualization and exploration of ensembles of contours or level sets of functions. Mirzargar et al. (2014) generalized the band depth for curves and proposed the curve boxplot. Hong et al. (2014) introduced a weighted functional boxplot for use when observations become shapes and images. Raj et al. (2017) proposed the graph-simplex band depth and developed a visualization tool called path boxplot. Yao et al. (2020) developed a trajectory functional boxplot (see Fig. 6) for visualization and exploratory analysis of trajectories that show variation in longitude and latitude through time.

The functional boxplot has some shortcomings, such as the loss of functional interpretation in the envelopes of the 50% central region and the non-outlying region and its inapplicability to functional observations under hidden temporal warping variability. Therefore, Xie et al. (2017) decomposed observation variation in functional data into three main components: amplitude, phase, and vertical translation based on curve

registration (Srivastava et al. 2011). They constructed a different visualization for each element based on the median, two quartiles, and extreme observations. They also proposed identifying outliers based on those three components and visualizing the amplitude or phase outliers through the phase-versus-amplitude distance plot.

4.2 Visualization based on decomposition

Another set of visualizations, specifically for outlier detection, is usually based on ranking criteria such as statistical depth or outlyingness. Due to the intrinsically infinite dimension, outliers contaminating functional data reveal various patterns. Regarding the amount of outlying proportion, they are divided as persistent or isolated outliers (Hubert et al. 2015); regarding whether they jump out of the normal range of oscillation, they are classified as magnitude or shape outliers (Dai et al. 2020). The outlier detection visualization tools that we introduce here can be separated into those specifically for univariate functional data and those for multivariate functional data (univariate functional data are usually special cases).

For univariate functional data, Arribas-Gil and Romo (2014) proposed using outliergrams to visualize and detect shape outliers in functional data by exploiting the relation between MBD and the modified epigraph index (MEI, López-Pintado and Romo 2011). Through a novel decomposition of the total variation depth, proposed by Huang and Sun (2019a), we can easily detect shape outliers via the boxplot of the modified shape similarity (MSS). Thereafter, the magnitude outliers can be seen among the remaining observations with the functional boxplots. Jiménez-Varón et al. (2024) proposed using pointwise depth to visualize magnitude and shape outliers, and the correlation between pairwise depths for shape outlier detection.

For multivariate functional data, Hubert et al. (2015) discussed amplitude and shape outliers and proposed various functional outlier maps based on the notion of outlyingness and depth in multivariate functional data, e.g., adjusted outlyingness (AO) and skew-adjusted projection depth (SPD). Furthermore, they exploited the relation between AO and SPD. They constructed the centrality–stability plot in which the amplitude outliers lie in the upper-right region and the shape outliers lie in the right region. Rousseeuw et al. (2018) proposed a robust notion of outlyingness, directional outlyingness (DO), and this can be applied in the univariate or multivariate setting. Based on the DO in the univariate setting, they defined the average of outlyingness as the functional directional outlyingness (FO) and measured the variability of its DO (VO). Then, they developed a graphical tool called the functional outlier map (FOM), which is a scatterplot of (FO, VO). Shift outliers, local outliers, and global outliers can be detected and displayed in different domains in FO. Based on the relation between mean directional outlyingness (MO) and VO, Dai and Genton (2018b) proposed a new graphical tool, the magnitude-shape (MS) plot, to illustrate the centrality of curves comprehensively. They also generalized the outliergram to the bivariate outliergram for outlier detection in bivariate functional data, according to a quadratic relation between FO and MO. However, the bivariate outliergram is limited to bivariate functional data and is less effective than the MS plot at measuring the centrality of curves. Yao et al. (2020) introduced wiggliness of directional outlyingness (WO)

to detect outliers and constructed the WO-MSBD plot which can distinguish shape outliers and magnitude outliers. The depth boxplot, introduced by Harris et al. (2021), is constructed on the elastic depths directly and serves as a half-boxplot. Its purpose is to identify potential amplitude and phase outliers. Ojo et al. (2023) proposed the magnitude–shape–amplitude (MSA) plot based on fast massive unsupervised outlier detection (FastMUOD, Ojo et al. 2022).

Plots visualizing the original curves provide more intuitive illustration of the data in the functional space, while plots visualizing the descriptive statistics provide more concise information within a low-dimensional space. In practice, one should combine the two types of visualization tools to get a more comprehensive understanding of the structure of the dataset of interest.

5 Functional clustering

In the terminology of machine learning, functional data clustering is an unsupervised learning process, partitioning similar observations into subgroups. The range of applications for functional data clustering is vast. For example, Abramowicz et al. (2017) applied a functional clustering method to study sediment data and to infer past environmental and climate changes. Athanasiadis and Mrkvička (2019) analyzed financial time series by using functional clustering methods to identify different insurance penetration (IP) rate profiles in European markets. In general, the resulting clusters show high potential for data visualization and interpretation.

When dealing with functional data, similarities might take into account the characteristics of the curves, such as their shapes, magnitudes, or derivatives (Hitchcock and Greenwood 2015). Broadly, we can classify the existing functional clustering methods as follows (Jacques and Preda 2014): 1) raw data methods; 2) filtering methods; 3) adaptive methods; and 4) distance-based methods. Raw data methods represent a naive approach and might result in high-dimensional vectorial clustering (Bouveyron and Brunet-Saumard 2014). Filtering methods and adaptive methods use the basis expansion approach for functional data with a common basis for all of the data or a common basis per group, respectively. The fundamental difference between filtering and adaptive methods (Cheam and Fredette 2020) lies in how the latter treats basis expansion coefficients and FPCA scores as random variables rather than parameters. Moreover, adaptive methods operate under the assumption that these random variables follow cluster-specific probability distributions. Some examples of clustering methods that use B-splines, Fourier basis, or functional principal component analysis have been described in detail by Abraham et al. (2003), Serban and Wasserman (2005), Chiou and Li (2007) and Shang (2014). Lastly, distance-based methods quantify the similarity between clusters by computing distances for functional observations. Here, we focus on distance-based methods. For a useful review of filtering and adaptive methods, we refer the reader to the articles by Jacques and Preda (2014) and Wang et al. (2016).

There are two main parts in a distance-based clustering method: the similarity measure and the clustering algorithm. We need to define a *similarity or dissimilarity measure* between curves that will be highly related to the interpretation of

the clusters. Usually, these measures are defined between two curves, $\{\boldsymbol{Y}_i, \boldsymbol{Y}_k\}$, where $\boldsymbol{Y}_i = (Y_i^{(1)}, \ldots, Y_i^{(p)})^\top$ and $\boldsymbol{Y}_k = (Y_k^{(1)}, \ldots, Y_k^{(p)})^\top$ are p-variate functional data, and we need a *clustering algorithm* to compute similarities across clusters, $C_1 = \{\boldsymbol{Y}_1^1, \ldots, \boldsymbol{Y}_{n_1}^1\}$ and $C_2 = \{\boldsymbol{Y}_1^2, \ldots, \boldsymbol{Y}_{n_2}^2\}$. Often, the similarity measure can be defined using a distance between functions, $d(\boldsymbol{Y}_i, \boldsymbol{Y}_k)$. Natural choices for the distance are the L_1, L_2, or L_∞ distances, where

$$d_l(\boldsymbol{Y}_i, \boldsymbol{Y}_k) = \left(\frac{1}{p} \sum_{j=1}^{p} \int_{\mathcal{T}_j} (|Y_i^{(j)}(t) - Y_k^{(j)}(t)|)^l \mathrm{d}t \right)^{1/l}$$

for $l = 1, 2$, and $d_\infty(\boldsymbol{Y}_i, \boldsymbol{Y}_k) = \max_{j=1,\ldots,p} \left(\frac{1}{p} \int_{\mathcal{T}_j} |Y_i^{(j)}(t) - Y_k^{(j)}(t)| \mathrm{d}t \right)$. The above distances are sensitive to both local and global changes in shape, allowing them to effectively capture the similarity between curves by measuring the extent of alignment between corresponding curves or by quantifying the maximum deviation along any component. If we consider the L_1, L_2, or L_∞ distance, then the resulting clusters are built of functions with similar shapes and magnitudes. If there is no interest in the similarity of magnitude, then the functions can be normalized and the total variation (TV) distance used (Alvarez-Esteban et al. 2016):

$$\begin{aligned} d_{TV}(\boldsymbol{Y}_i, \boldsymbol{Y}_k) &= 1 - \frac{1}{p} \sum_{j=1}^{p} \int_{\mathcal{T}_j} \min\{Y_i^{(j)}(t), Y_k^{(j)}(t)\} \mathrm{d}t \\ &= \frac{1}{2p} \sum_{j=1}^{p} \int_{\mathcal{T}_j} |Y_i^{(j)}(t) - Y_k^{(j)}(t)| \mathrm{d}t. \end{aligned}$$

These distances might be further enhanced by including information about the derivative curves and defining a similarity measure as a weighted combination of the distances as discussed by Jacques and Preda (2014).

Here, we assume that the curves $\boldsymbol{Y}_i's$ are all independent. However, if the user is interested in clustering dependent curves, then a similarity measure can be proposed that uses the Spearman correlation or the rank correlation between functions (Heckman and Zamar 2000). If these curves are linked to a time series trajectory, then a coherence-based distance might be useful too (Euán et al. 2019). In this setting, the correlation of the resulting clusters is high within each group but low across clusters. Chen et al. (2021) introduced two novel robust rank-based dissimilarity measures: one based on the distance between functional medians and the other based on the size of the central region during merging. Dai et al. (2021) induced the dissimilarity matrix from functional ordering. The idea is to construct the set of functional differences, apply any functional depth (or ranking) notions to the above set, and define the similarity as one minus the depth.

However, those methods assume that functions are observed at a fixed set of points, and no sparseness exists. Elastic time distance was proposed by Qu et al. (2025) to address this issue. It is applicable to (multivariate) functional data with either iden-

tical or different time measurements per subject. The core idea is to build standard grid points ($[t_1, t_2, \ldots, t_T]$, where $t_m \in \mathcal{T} \subset \mathbb{R}$ for $m = 1, \ldots, T$) and to interpolate measurements at standard grid points with the available observations. Assume curves $\boldsymbol{Y}_i$ and $\boldsymbol{Y}_k$ are p-variate multivariate functional data and that $\widetilde{\boldsymbol{Y}}_i$ and $\widetilde{\boldsymbol{Y}}_k$ are their interpolated observations based on procedures described by Qu et al. (2025), then

$$d_{ETD}(\boldsymbol{Y}_i, \boldsymbol{Y}_k) = \max_{m=1,\ldots,T} \sqrt{\sum_{j=1}^{p} \{\widetilde{Y}_i^{(j)}(t_m) - \widetilde{Y}_k^{(j)}(t_m)\}^2}, \quad t_m \in \mathcal{T}.$$

Once the similarity measure is chosen, we use a clustering algorithm that selects the groups of functions that are more similar in an "optimal" manner, i.e., members within each group are highly similar, but members across groups are highly dissimilar. The algorithms most commonly used for this purpose are the k-means and hierarchical clustering algorithms. Ferraty et al. (2006) introduced examples of hierarchical clustering using the L_2 distance between the functions and their second derivatives. Ieva et al. (2013) applied a k-means to identify clusters of electrocardiograph traces with a weighted distance between the curves and their first derivatives. Recently, Euán et al. (2018) proposed the hierarchical merger clustering algorithm. Its main contribution to classical hierarchical algorithms is the use of a representative member for each cluster. Euán et al. (2018) proposed using the TV distance in a hierarchical merger algorithm to cluster spectral density functions from ocean wave time series. Euán and Sun (2019) extended this method to general 2D directional spectra functions. Moreover, Qu et al. (2025) proposed the robust two-layer partition (RTLP) clustering algorithm and combined it with the elastic time distance to cluster multivariate functional curves. They also compared RTLP clustering with other algorithms, including the distance-based methods DBSCAN, k-means, and k-medians, and the model-based funHDDC algorithm (Schmutz et al. 2020).

Some real data applications might need a more robust clustering algorithm, especially if the data have a high noise level. Although some of the methods described previously in this section might separate possible outliers as single clusters, this is not true for all methods. In the presence of potential outliers, Cuesta-Albertos and Fraiman (2007) proposed a trimmed k-means clustering that results in a robust cluster procedure for functional data. Also, Rivera-García et al. (2019) applied the trimming technique to introduce a robust model-based clustering method for functional data. When data are misaligned, applying clustering methods directly might result in non-reasonable clustering structures. Sangalli et al. (2010) proposed an algorithm that considers the case in which curves are misaligned. De Micheaux et al. (2021), based on the curve depth, employed the original clustering algorithm (Jörnsten 2004) with slight modifications for unparameterized curves. The robust two-layer partition clustering, introduced by Qu et al. (2025), uses both a two-layer partition algorithm and a modified silhouette index. This approach is effective at distinguishing clusters and identifying potential outliers in terms of their magnitude and shape.

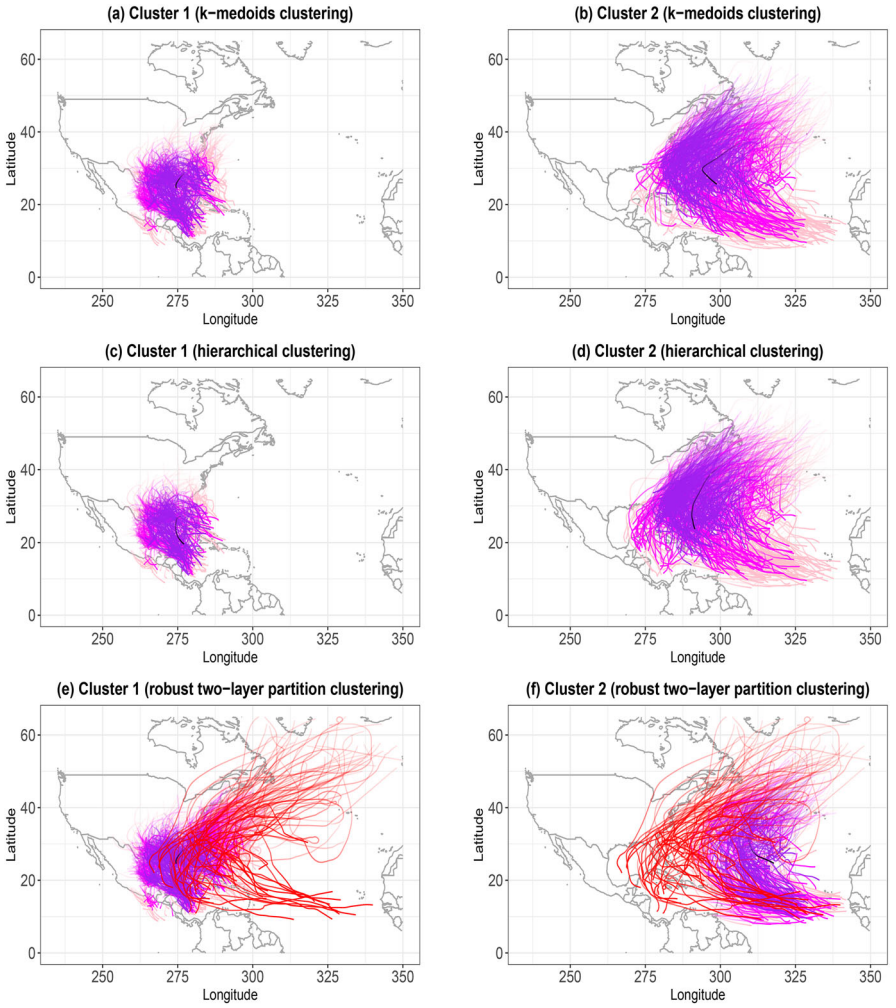

Fig. 6 North Atlantic cyclone track clusters visualized with our version of the trajectory functional boxplot (Yao et al. 2020). (**a**) and (**b**) are from k-medoids clustering, (**c**) and (**d**) are from hierarchical clustering, and (**e**) and (**f**) are from robust two-layer partition clustering. Black and red represent the median and outliers, respectively, and purple, magenta, and pink indicate the first, second, and third quartile curves, respectively

In general, a good strategy is to select the clustering method based on the research goal. We illustrate this by using the bivariate hurricane trajectory data for the North Atlantic, see Fig. 1 (b). Because the trajectory data have various observations per subject, we apply the elastic time distance mentioned in Qu et al. (2025) and consider the following different clustering methods based on the interpolated data: 1) k-medoids clustering (Park and Jun 2009), see Fig. 6 (a)-(b); 2) hierarchical clustering with the average as the linkage function, see Fig. 6 (c)-(d); and 3) robust two-layer partition clustering, see Fig. 6 (e)-(f). Each clustering method generates two clusters, but outliers are introduced only by the robust two-layer partition clustering.

6 Discussion

We have presented an overview of methods and tools to perform exploratory functional data analysis (EFDA) and broadened its scope from analyzing only fully observed univariate functional data to encompassing irregular multivariate functional data. By using functional depths and distances, EFDA offers a wide array of tools for visualizing and clustering both dense and sparse multivariate functional data, and for detecting outliers.

Functional depths play a pivotal role in establishing functional rankings, forming the foundation for generating functional boxplots and identifying outliers. According to the method of obtaining depth values, these functional depths can be categorized into three types. The first type is referred to as the integral depth that takes as values the average pointwise depths or sample-wise distances, e.g., (modified) band depth (López-Pintado and Romo 2009), (modified) simplicial band depth (López-Pintado et al. 2014), and L^∞ depth (Long and Huang 2015). The second type is infimal depth which takes the minimum instead of the average of the above quantities, and examples include random projection depth (Cuevas et al. 2007) and the depths described by Mosler (2013). These two types first map each functional observation to a scalar and then ranks them according to the resultant scalars. In contrast, the third type of depths first gets global ranking of the observations and calculates the depth according to the ranking result. Typical examples of this type include global envelop depth (Myllymäki et al. 2017) and extremal depth (Narisetty and Nair 2016).

Applying functional depths to sparse functional data is more complex because of the irregular coordinate grids. One approach to address this issue involves estimating curves and their confidence bands or, alternatively, applying global functional depth to sparse functional data directly as proposed by Qu et al. (2022). The original functional boxplot serves to identify central tendencies and outliers. However, it has limitations with regard to detecting certain shape outliers, and it may not be directly applicable to functional data with missing values. To address these limitations, variations of functional boxplots and other visualization tools have been proposed, enabling the detection of shape outliers and facilitating the application to sparse functional data.

Moreover, functional distances play a crucial role in functional clustering. Examples of such distances include the L_p distance, the total variation distance, and the elastic time distance. By leveraging functional distances, a wide range of classical clustering algorithms, as well as novel ones, can be applied to functional data. To handle common noise present in real-world data, robust two-layer partition clustering techniques can effectively separate potential outliers from the clusters.

Although this review has extended its domain from classical functional data to sparse multivariate functional data, a wider area of functional data can be considered, and this may pose new challenges in visualization, robust statistics, and clustering. New-generation functional data can include: functional snippets (Lin and Wang 2022, see longitudinal measurements of spinal bone mineral density for healthy subjects with at least 2 measurements); functional time series data, e.g., functional ACF and PACF plots (Mestre et al. 2021), calendar-based graphics (Wang et al. 2020), surface time series (Martínez-Hernández and Genton 2023), and functional records (Martínez-Hernández and Genton 2025); interval-valued functional data (Nasirzadeh et al. 2022,

see the simultaneous systolic and diastolic blood pressure of patients at different visit times); longitudinal functional data from a clinical trial (see the medical imaging data of patients at different time points during a clinical study in the papers by Adeli et al. 2019 and Zhu et al. 2021); spatial functional data (Delicado et al. 2010; see the longitudinal climate data from arrays of monitors in the nearby area, and the review by Martínez-Hernández and Genton 2020), and wearable health data (Smets et al. 2018).

References

Abraham C, Cornillon PA, Matzner-Løber E, Molinari N (2003) Unsupervised curve clustering using b-splines. Scandinavian J Statistics 30(3):581–595

Abramowicz K, Arnqvist P, Secchi P, Sjöstedt de Luna S, Vantini S, Vitelli V (2017) Clustering misaligned dependent curves applied to varved lake sediment for climate reconstruction. Stochastic Environ Res Risk Asses 31(1):71–85

Adeli E, Meng Y, Li G, Lin W, Shen D (2019) Multi-task prediction of infant cognitive scores from longitudinal incomplete neuroimaging data. Neuro Image 185:783–792

Allen TT (2019) Introduction to Engineering Statistics and Lean Six Sigma: Statistical Quality Control and Design of Experiments and Systems, vol 3. Springer

Alvarez-Esteban PC, Euán C, Ortega J (2016) Time series clustering using the total variation distance with applications in oceanography. Environ 27(6):355–369

Arribas-Gil A, Romo J (2014) Shape outlier detection and visualization for functional data: the outliergram. Biostatistics 15(4):603–619

Athanasiadis S, Mrkvička T (2019). European insurance market analysis: A multivariate clustering approach. In *Proceedings of the 12th International Scientific Conference INPROFORUM* (pp. 328–333)

Berrendero JR, Justel A, Svarc M (2011) Principal components for multivariate functional data. Computational Statistics & Data Analysis 55(9):2619–2634

Bouveyron C, Brunet-Saumard C (2014) Model-based clustering of high-dimensional data: A review. Computational Statistics & Data Analysis 71:52–78

Cai T, Yuan M (2010). Nonparametric covariance function estimation for functional and longitudinal data. *Technical report, University of Pennsylvania and Georgia Institute of Technology*

Carroll C, Müller H-G, Kneip A (2021) Cross-component registration for multivariate functional data, with application to growth curves. Biometrics 77(3):839–851

Castruccio S, Genton MG, Sun Y (2019) Visualizing spatiotemporal models with virtual reality: From fully immersive environments to applications in stereoscopic view. J Royal Statistical Society: Series A 182(2):379–387

Chang W, Cheng J, Allaire J, Xie Y, McPherson J (2015). Package 'shiny'. *https://cran.r-project.org/web/packages/shiny/shiny.pdf*

Cheam AS, Fredette M (2020) On the importance of similarity characteristics of curve clustering and its applications. Pattern Recognition Letters 135:360–367

Chen T, Sun Y, Euan C, Ombao H (2021) Clustering brain signals: A robust approach using functional data ranking. J Classification 38:425–442

Chiou J-M, Li P-L (2007) Functional Clustering and Identifying Substructures of Longitudinal Data. J Royal Statistical Society Series B: Statistical Methodology 69(4):679–699

Claeskens G, Hubert M, Slaets L, Vakili K (2014) Multivariate functional halfspace depth. J American Statistical Association 109(505):411–423

Crainiceanu C, Reiss P, Goldsmith J, Huang L, Huo L, Scheipl F, Swihart B, Greven S, Harezlak J, Kundu MG, Zhao Y, Mclean M, Xiao L (2013). Package 'refund'. https://cran.r-project.org/web/packages/refund/refund.pdf

Cuesta-Albertos JA, Fraiman R (2007) Impartial trimmed K-means for functional data. Computational Statistics & Data Analysis 51(10):4864–4877

Cuevas A, Febrero M, Fraiman R (2007) Robust estimation and classification for functional data via projection-based depth notions. Computational Statistics 22(3):481–496

Dai W, Athanasiadis S, Mrkvička T (2021). A new functional clustering method with combined dissimilarity sources and graphical interpretation. In *Computational Statistics and Applications* (pp. 3–23). IntechOpen

Dai W, Genton MG (2018) Functional boxplots for multivariate curves. Stat 7(1):e190

Dai W, Genton MG (2018) Multivariate functional data visualization and outlier detection. J Computational and Graphical Statistics 27(4):923–934

Dai W, Genton MG (2019) Directional outlyingness for multivariate functional data. Computational Statistics & Data Analysis 131:50–65

Dai W, Mrkvička T, Sun Y, Genton MG (2020) Functional outlier detection and taxonomy by sequential transformations. Computational Statistics & Data Analysis 149:106960

De Micheaux PL, Mozharovskyi P, Vimond M (2021) Depth for curve data and applications. J American Statistical Association 116(536):1881–1897

Delicado P, Giraldo R, Comas C, Mateu J (2010) Statistics for spatial functional data: some recent contributions. Environmetrics 21(3–4):224–239

Elías A, Jiménez R, Paganoni AM, Sangalli LM (2023) Integrated depths for partially observed functional data. J Computational and Graphical Statistics 32(2):341–352

Euán C, Ombao H, Ortega J (2018) The hierarchical spectral merger algorithm: A new time series clustering procedure. J Classification 35(1):71–99

Euán C, Sun Y (2019) Directional spectra-based clustering for visualizing patterns of ocean waves and winds. J Computational and Graphical Statistics 28(3):659–670

Euán C, Sun Y, Ombao H (2019) Coherence-based time series clustering for statistical inference and visualization of brain connectivity. Annals of Applied Statistics 13(2):990–1015

Fan J, Gijbels I (1996) Local Polynomial Modelling and Its Applications, vol 66. CRC Press, Monographs on Statistics and Applied Probability

Ferraty F, Vieu P (2006). *Nonparametric Functional Data Analysis: Theory and Practice*. Springer

Fraiman R, Muniz G (2001) Trimmed means for functional data. TEST 10:419–440

Friedman JH, Stuetzle W, John W (2002) Tukey's work on interactive graphics. The Annals of Statistics 30(6):1629–1639

Genton MG, Castruccio S, Crippa P, Dutta S, Huser R, Sun Y, Vettori S (2015) Visuanimation in statistics. Stat 4(1):81–96

Genton MG, Johnson C, Potter K, Stenchikov G, Sun Y (2014) Surface boxplots. Stat 3(1):1–11

Genton MG, Sun Y (2020). Functional data visualization. *In Wiley StatsRef: Statistics Reference Online, Davidian, M., Kenett, R. S., Longford, N. T., Molenberghs, G., Piegorsch, W. W., and Ruggeri, F. (eds)*, (pp. 1–11)

Happ C, Greven S (2018) Multivariate functional principal component analysis for data observed on different (dimensional) domains. J American Statistical Association 113(522):649–659

Hardin J, Rocke DM (2005) The distribution of robust distances. J Computational and Graphical Statistics 14:928–946

Harris T, Tucker JD, Li B, Shand L (2021) Elastic depths for detecting shape anomalies in functional data. Technometrics 63(4):466–476

Heckman N, Zamar R (2000) Comparing the shapes of regression functions. Biometrika 87(1):135–144

Hitchcock DB, Greenwood MC (2015). Clustering functional data. In *Handbook of Cluster Analysis* chapter 13, (pp. 265–287). Chapman and Hall/CRC

Hong Y, Davis B, Marron J, Kwitt R, Singh N, Kimbell JS, Pitkin E, Superfine R, Davis SD, Zdanski CJ et al (2014) Statistical atlas construction via weighted functional boxplots. Medical Image Analysis 18(4):684–698

Horváth L, Kokoszka P (2012) Inference for Functional Data with Applications. Springer

Hsing T, Eubank R (2015) Theoretical Foundations of Functional Data Analysis, with an Introduction to Linear Operators, vol 997. John Wiley & Sons

Huang H, Sun Y (2019) A decomposition of total variation depth for understanding functional outliers. Technometrics 61(4):445–458

Huang H, Sun Y (2019) Visualization and assessment of spatio-temporal covariance properties. Spatial Statistics 34:100272

Huang H, Sun Y, Genton MG (2023) Test and visualization of covariance properties for multivariate spatio-temporal random fields. J Computational and Graphical Statistics 32:1545–1555

Hubert M, Rousseeuw PJ, Segaert P (2015) Multivariate functional outlier detection. Statistical Methods & Applications 24(2):177–202

Hyndman RJ (1996) Computing and graphing highest density regions. The American Statistician 50(2):120–126
Hyndman RJ, Shang HL (2010) Rainbow plots, bagplots, and boxplots for functional data. J Computational and Graphical Statistics 19(1):29–45
Ieva F, Paganoni AM (2013) Depth measures for multivariate functional data. Communications in Statistics-Theory and Methods 42(7):1265–1276
Ieva F, Paganoni AM, Pigoli D, Vitelli V (2013) Multivariate functional clustering for the morphological analysis of electrocardiograph curves. J Royal Statistical Society: Series C (Applied Statistics) 62(3):401–418
Jacques J, Preda C (2014) Functional data clustering: a survey. Adv Data Analysis and Classification 8(3):231–255
Jiménez-Varón CF, Lee H, Genton MG, Sun Y (2023). Visualization and assessment of copula symmetry. arXiv 2312.10675
Jiménez-Varón CF, Harrou F, Sun Y (2024) Pointwise data depth for univariate and multivariate functional outlier detection. Environmetrics 35(5):e2851
Jörnsten R (2004) Clustering and classification based on the L1 data depth. J Multivariate Analysis 90(1):67–89
Kuhnt S, Rehage A (2016) An angle-based multivariate functional pseudo-depth for shape outlier detection. J Multivariate Analysis 146:325–340
Li C, Xiao L, Luo S (2020) Fast covariance estimation for multivariate sparse functional data. Stat 9(1):e245
Lin Z, Wang J-L (2022) Mean and covariance estimation for functional snippets. J American Statistical Association 117(537):348–360
Long JP, Huang JZ (2015). A study of functional depths. *arXiv preprint* arXiv:1506.01332
López-Pintado S, Romo J (2009) On the concept of depth for functional data. J American Statistical Association 104(486):718–734
López-Pintado S, Romo J (2011) A half-region depth for functional data. Computational Statistics & Data Analysis 55(4):1679–1695
López-Pintado S, Sun Y, Lin JK, Genton MG (2014) Simplicial band depth for multivariate functional data. Adv Data Analysis and Classification 8:321–338
López-Pintado S, Wei Y (2011). Depth for sparse functional data. In *Recent Advances in Functional Data Analysis and Related Topics* (pp. 209–212).: Springer
López-Pintado S, Wrobel J (2017) Robust non-parametric tests for imaging data based on data depth. Stat 6(1):405–419
Martínez-Hernández I, Genton MG (2020) Recent developments in complex and spatially correlated functional data. Brazilian J Probability and Statistics 34(2):204–229
Martínez-Hernández I, Genton MG (2023). Surface time series models for large spatio-temporal datasets. Spatial Statistics, 53, Paper No. 100718, 16
Martínez-Hernández I, Genton MG (2025). Functional time series analysis and visualization based on records. J Computational and Graphical Statistics, (pp. to appear)
Mestre G, Portela J, Rice G, Roque Muñoz San A, Alonso E (2021) Functional time series model identification and diagnosis by means of auto- and partial autocorrelation analysis. Computational Statistics & Data Analysis 155:107108
Mirzargar M, Whitaker RT, Kirby RM (2014) Curve boxplot: Generalization of boxplot for ensembles of curves. IEEE Transactions on Visualization and Computer Graphics 20(12):2654–2663
Mosler K (2013). *Depth Statistics*, (pp. 17–34). Springer Berlin Heidelberg: Berlin, Heidelberg
Myllymäki M, Mrkvička T (2019). GET: Global envelopes in R. *arXiv preprint* arXiv:1911.06583
Myllymäki M, Mrkvička T, Grabarnik P, Seijo H, Hahn U (2017) Global envelope tests for spatial processes. J Royal Statistical Society: Series B 79(2):381–404
Nagy S, Gijbels I, Hlubinka D (2017) Depth-based recognition of shape outlying functions. J Computational and Graphical Statistics 26(4):883–893
Narisetty NN, Nair VN (2016) Extremal depth for functional data and applications. J American Statistical Association 111(516):1705–1714
Nasirzadeh R, Nasirzadeh F, Mohammadi Z (2022) Some non-parametric regression models for interval-valued functional data. Stat 11(1):e443
Ojo OT, Fernández Anta A, Genton MG, Lillo RE (2023) Multivariate functional outlier detection using the fast massive unsupervised outlier detection indices. Stat 12(1):e567

Ojo OT, Fernández Anta A, Lillo RE, Sguera C (2022) Detecting and classifying outliers in big functional data. Adv in Data Analysis and Classification 16(3):725–760
Park H-S, Jun C-H (2009) A simple and fast algorithm for k-medoids clustering. Expert Systems with Applications 36(2):3336–3341
Parkinson J, Minton J, Bouttell J, Lewsey J, Shah A, McCartney G (2020) Do age, period or cohort effects explain circulatory disease mortality trends, scotland 1974–2015? Heart 106(8):584–589
Qu Z, Dai W, Genton MG (2021) Robust functional multivariate analysis of variance with environmental applications. Environmetrics 32(1):e2641
Qu Z, Dai W, Genton MG (2022). Global depths for irregularly observed multivariate functional data. *arXiv preprint* arXiv:2211.15125
Qu Z, Dai W, Genton MG (2025) Robust two-layer partition clustering of sparse multivariate functional data. In press, Econometrics and Statistics
Qu Z, Genton MG (2022) Sparse functional boxplots for multivariate curves. J Computational and Graphical Statistics 31(4):976–989
Raj M, Mirzargar M, Ricci R, Kirby RM, Whitaker RT (2017) Path boxplots: a method for characterizing uncertainty in path ensembles on a graph. J Computational and Graphical Statistics 26(2):243–252
Ramsay J, Hooker G, Graves S (2009). Introduction to functional data analysis. In *Functional data analysis with R and MATLAB* (pp. 1–19). Springer
Ramsay J, Wickham H, Graves S, Hooker G (2023). Package 'fda'. https://cran.r-project.org/web/packages/fda/fda.pdf
Ramsay JO, Dalzell C (1991) Some tools for functional data analysis. J Royal Statistical Society: Series B (Methodological) 53(3):539–561
Ramsay JO, Silverman BW (2005). *Functional Data Analysis* (second ed.).Springer
Rivera-García D, García-Escudero LA, Mayo-Iscar A, Ortega J (2019) Robust clustering for functional data based on trimming and constraints. Adv in Data Analysis and Classification 13(1):201–225
Rousseeuw PJ (1985). Multivariate estimation with high breakdown point. In *Mathematical Statistics and Applications, Volume B* (W. Grossmann, G. Pflug, I. Vincze and W. Wert, eds.) (pp. 283–297). Reidel, Dordrecht
Rousseeuw PJ, Raymaekers J, Hubert M (2018) A measure of directional outlyingness with applications to image data and video. J Computational and Graphical Statistics 27(2):345–359
Rousseeuw PJ, Ruts I, Tukey JW (1999) The bagplot: a bivariate boxplot. The American Statistician 53(4):382–387
Sangalli LM, Secchi P, Vantini S, Veneziani A (2009) A case study in exploratory functional data analysis: geometrical features of the internal carotid artery. J American Statistical Association 104(485):37–48
Sangalli LM, Secchi P, Vantini S, Vitelli V (2010) K-mean alignment for curve clustering. Computational Statistics & Data Analysis 54(5):1219–1233
Schmutz A, Jacques J, Bouveyron C, Cheze L, Martin P (2020) Clustering multivariate functional data in group-specific functional subspaces. Computational Statistics 35(3):1101–1131
Serban N, Wasserman L (2005) Cats: Clustering after transformation and smoothing. J American Statistical Association 100(471):990–999
Serfling R, Wijesuriya U (2017) Depth-based nonparametric description of functional data, with emphasis on use of spatial depth. Computational Statistics & Data Analysis 105:24–45
Sguera C, López-Pintado S (2021) A notion of depth for sparse functional data. TEST 30(3):630–649
Shang HL (2014) A survey of functional principal component analysis. AStA Adva in Statistical Analysis 98:121–142
Shang HL, Hyndman RJ (2017) Grouped functional time series forecasting: An application to age-specific mortality rates. J Computational and Graphical Statistics 26(2):330–343
Shang HL, Hyndman RJ (2019). Package 'rainbow'. *R packages*, 43. https://cran.r-project.org/web/packages/rainbow/rainbow.pdf
Sievert C, Hocking T, Chamberlain S, Ram K, Corvellec M, Despouy P (2018). plotly for R. https://cran.r-project.org/web/packages/plotly/plotly.pdf
Smets E, Rios Velazquez E, Schiavone G, Chakroun I, D'Hondt E, De Raedt W, Cornelis J, Janssens O, Van Hoecke S, Claes S et al (2018) Large-scale wearable data reveal digital phenotypes for daily-life stress detection. NPJ Digital Medicine 1(1):67
Srivastava A, Wu W, Kurtek S, Klassen E, Marron JS (2011). Registration of functional data using Fisher-Rao metric. *arXiv preprint* arXiv:1103.3817
Sun Y, Genton MG (2011) Functional boxplots. J Computational and Graphical Statistics 20(2):316–334

Sun Y, Genton MG (2012) Adjusted functional boxplots for spatio-temporal data visualization and outlier detection. Environmetrics 23(1):54–64
Sun Y, Genton MG (2012) Functional median polish. J Agricultural, Biological, and Environmental Statistics 17:354–376
Sun Y, Genton MG, Nychka DW (2012) Exact fast computation of band depth for large functional datasets: How quickly can one million curves be ranked? Stat 1:68–74
Tukey JW (1975). Mathematics and the picturing of data. In *Proceedings of the International Congress of Mathematicians*, volume 2 (pp. 523–531)
Tukey JW (1977) *Exploratory Data Analysis*, vol 2. Addison-Wesley, Reading, MA, USA
Tukey JW (1980) We need both exploratory and confirmatory. The American Statistician 34(1):23–25
Wand MP, Jones MC (1995) *Kernel Smoothing*. Chapman and Hall, London
Wang E, Cook D, Hyndman RJ (2020) Calendar-based graphics for visualizing people's daily schedules. J Computational and Graphical Statistics 29(3):490–502
Wang JL, Chiou JM, Müller HG (2016) Functional data analysis. Annual Review of Statistics and Its Application 3:257–295
Wang Y (2011) *Smoothing Splines: Methods and Applications*. Chapman and Hall, New York
Whitaker RT, Mirzargar M, Kirby RM (2013) Contour boxplots: A method for characterizing uncertainty in feature sets from simulation ensembles. IEEE Transactions on Visualization and Computer Graphics 19(12):2713–2722
Wrobel J, Goldsmith J (2022). refund.shiny: Interactive Plotting for Functional Data Analyses. R package version 1.0. https://cran.r-project.org/web/packages/refund.shiny/refund.shiny.pdf
Wrobel J, Park SY, Staicu AM, Goldsmith J (2016) Interactive graphics for functional data analyses. Stat 5(1):108–118
Wu Z, Euán C, Crujeiras RM, Sun Y (2023) Estimation and clustering of directional wave spectra. J Agricultural, Biological and Environmental Statistics 28:502–525
Xiao L, Li C, Checkley W, Crainiceanu C (2018) Fast covariance estimation for sparse functional data. Statistics and Computing 28:511–522
Xie W, Kurtek S, Bharath K, Sun Y (2017) A geometric approach to visualization of variability in functional data. J American Statistical Association 112(519):979–993
Yao F, Müller HG, Wang JL (2005) Functional linear regression analysis for longitudinal data. The Annals of Statistics 33(6):2873–2903
Yao Z, Dai W, Genton G, M. G. (2020) Trajectory functional boxplots. Stat 9(1):e289
Zhao X, Marron J, Wells MT (2004) The functional data analysis view of longitudinal data. Statistica Sinica 14(2004):789–808
Zhu Y, Kim M, Zhu X, Kaufer D, Wu G, Initiative ADN et al (2021) Long range early diagnosis of Alzheimer's disease using longitudinal MR imaging data. Medical Image Analysis 67:101825